Mitochondrial Cholesterol Contributes to Chemotherapy Resistance in Hepatocellular Carcinoma

Joan Montero,[1,2] Albert Morales,[1,2] Laura Llacuna,[1,2] Josep M. Lluis,[1,2] Oihana Terrones,[3] Gorka Basañez,[3] Bruno Antonsson,[4] Jesús Prieto,[2,5] Carmen García-Ruiz,[1,2] Anna Colell,[1,2] and José C. Fernández-Checa[1,2]

[1]Liver Unit and Centro de Investigaciones Biomédicas Esther Koplowitz, IMDiM, Hospital Clínic i Provincial, Institut d'Investigacions Biomèdiques August Pi i Sunyer, and Department of Cell Death and Proliferation, Instituto de Investigaciones Biomédicas de Barcelona, Consejo Superior de Investigaciones Científicas, Barcelona, Spain; [2]Centro de Investigación Biomédica en Red (CIBERehd); [3]Unidad de Biofísica (Centro Mixto Consejo Superior de Investigaciones Científicas-Universidad del País Vasco/Euskal Herriko Unibertsitatea), Universidad del País Vasco/Euskal Herriko Unibertsitatea, Bilbao, Spain; [4]Merck Serono Internacional, Geneva, Switzerland; and [5]Liver Unit and Division of Hepatology and Gene Therapy, University Clinic and Center for Applied Medical Research, University of Navarra, Pamplona, Spain

Abstract

Cholesterol metabolism is deregulated in carcinogenesis, and cancer cells exhibit enhanced mitochondrial cholesterol content whose role in cell death susceptibility and cancer therapy has not been investigated. Here, we describe that mitochondria from rat or human hepatocellular carcinoma (HC) cells (HCC) or primary tumors from patients with HC exhibit increased mitochondrial cholesterol levels. HCC sensitivity to chemotherapy acting via mitochondria is enhanced upon cholesterol depletion by inhibition of hydroxymethylglutaryl-CoA reductase or squalene synthase (SS), which catalyzes the first committed step in cholesterol biosynthesis. HCC transfection with siRNA targeting the steroidogenic acute regulatory protein StAR, a mitochondrial cholesterol–transporting polypeptide which is overexpressed in HCC compared with rat and human liver, sensitized HCC to chemotherapy. Isolated mitochondria from HCC with increased cholesterol levels were resistant to mitochondrial membrane permeabilization and release of cytochrome *c* or Smac/DIABLO in response to various stimuli including active Bax. Similar behavior was observed in cholesterol-enriched mitochondria or liposomes and reversed by restoring mitochondrial membrane order or cholesterol extraction. Moreover, atorvastatin or the SS inhibitor YM-53601 potentiated doxorubicin-mediated HCC growth arrest and cell death *in vivo*. Thus, mitochondrial cholesterol contributes to chemotherapy resistance by increasing membrane order, emerging as a novel therapeutic niche in cancer therapy. [Cancer Res 2008;68(13):5246–56]

Introduction

Cholesterol is an integral component of cellular membranes that plays an essential role in maintaining their integrity and function (1). In addition to the regulation of membrane order, cholesterol induces membrane packing in lateral microdomains (rafts) of the plasma membrane, providing a scaffold for a variety of membrane-associated signaling proteins (2, 3). Due to this role in modulating membrane structure and function, cholesterol levels in cell membranes are tightly regulated. The main sources of cellular cholesterol involve either its uptake from cholesterol-rich low-density lipoproteins or its *de novo* synthesis through the conversion of 3-hydroxy-3-methylglutaryl-CoA into mevalonate by 3-hydroxy-3-methylglutaryl CoA reductase (HMG-CoAR), the rate-limiting step in cholesterol synthesis, which is transcriptionally regulated by endoplasmic reticulum–based transcription factor SREBP-2 (1, 4).

Cholesterol accumulation and enhanced cholesterol-rich lipid rafts have been reported in several solid tumors that modulate tumor cell growth and survival by activating particular signaling pathways such as Akt (5, 6). In addition, cholesterol metabolism is abnormal in many malignancies with loss of cholesterol feedback and HMG-CoAR up-regulation despite enhanced cholesterol levels (7). Moreover, malignant cells exhibit elevated levels of mevalonate, which has been shown to promote tumor growth *in vivo* and proliferation of breast cancer cells (8). Consistent with this scenario, statins, which block HMG-CoAR by competing with mevalonate for binding to the active site, have been proposed for cancer prevention and/or treatment, although their efficacy as anticancer agents has not always been established (9). Furthermore, even in those cases where statins showed promising results, it remained unclear whether the therapeutic effects were due to the cholesterol-lowering activity or to the down-regulation of isoprenoids, which are known to modulate multiple proteins by posttranslational modifications (9, 10).

Mitochondria are cholesterol-poor organelles with estimates ranging from 0.5% to 3% of the content found in plasma membranes (1, 11). However, unphysiologic mitochondrial cholesterol levels have been described in solid tumors. For instance, mitochondrial cholesterol levels of tumors from Buffalo rats bearing transplanted Morris hepatomas were 2- to 5-fold higher than the content found in mitochondria prepared from host liver, and correlated with the degree of tumor growth and malignancy (12–15). Although the mechanisms underlying the mitochondrial cholesterol accumulation in cancer cells are poorly understood, recent observations have reported the activity of cholesterol-transporting polypeptides, including the steroidogenic acute regulatory protein (StAR) in human HepG2 cells that contribute to the mitochondrial intermembrane trafficking of cholesterol (16). Although cholesterol enrichment in mitochondria can impair specific mitochondrial components accounting, in part, for the mitochondrial dysfunction described in cancer cells (13, 15, 17–20),

Note: Supplementary data for this article are available at Cancer Research Online (http://cancerres.aacrjournals.org/).

A. Colell and J.C. Fernández-Checa share senior authorship.

Requests for reprints: José C. Fernández-Checa, Liver Unit, Hospital Clínic i Provincial, C/Villarroel, 170, 08036-Barcelona, Spain. Phone: 34-93-227-5709; Fax: 34-93-451-5272; E-mail: checa229@yahoo.com.

doi:10.1158/0008-5472.CAN-07-6161

its effect in cell death susceptibility and cancer therapy has not been previously examined. This may be of potential relevance because strategies targeting mitochondria have been proposed as potential use in cancer therapy (21), and alterations in the mitochondrial apoptotic pathway, particularly the modulation of the mitochondrial membrane permeabilization (MMP), may contribute to cancer growth and desensitization to cancer therapy (21, 22).

Hepatocellular carcinoma (HC) is one of the main causes of cancer-related deaths that frequently arises on a background of chronic inflammation and exhibits high resistance to current therapy (23). Thus, because mitochondria are known to play a key role in cell death (22) and cholesterol-regulated mitochondrial membrane order has been reported to modulate MMP and the subsequent release of apoptotic proteins (19), the purpose of this study was to examine the role of mitochondrial cholesterol in the susceptibility of HC cells (HCC) to chemotherapy *in vitro*, the mechanisms involved, and the relevance in an *in vivo* HC model. Our findings indicate that mitochondrial cholesterol contributes to chemotherapy resistance through altered membrane order, hence emerging as a novel therapeutic target in cancer therapy.

Materials and Methods

Materials and recombinant proteins. Dioleoylphosphatidylcholine, tetraoleoylcardiolipin, and cholesterol were purchased from Avanti Polar Lipids. Dodecyl octaethylene glycol monoether ($C_{12}E_8$), Methyl-β-cyclodextrin, melittin, *Staphylococcus aureus* α-toxin, tetanolysin, and fluoresceinisothiocyanate-labeled dextrans of 70 kDa (FD-70) were obtained from Sigma. Recombinant full-length human Bax with an amino-terminal His6 tag (Bax), caspase 8–cleaved murine BID with an amino-terminal His6 tag (tBid), and human Bcl-2 lacking the carboxy-terminal hydrophobic domain (Bcl-2DC) were purified as previously described (24). Oligomeric Bax (oligo-Bax) was obtained by incubating Bax in 100 mmol/L KCl, 10 mmol/L HEPES, 0.1 mmol/L EDTA (pH 7.0) buffer (KHE buffer) containing octylglucoside (2%, w/v) for 1 h at 4°C.

Cell culture, hepatocyte isolation, and mitochondria and mitoplasts preparation. The human hepatoblastoma cell line, HepG2, and the rat hepatoma cell line, Reuber H35, were both obtained from the European Collection of Animal Cell Cultures and grown at 37°C in 5% CO_2. Culture medium was supplemented with 10% fetal bovine serum (FBS), 2 mmol/L L-glutamine, and 1% nonessential amino acids and antibiotics. In some experiments, 10% of delipidated FBS was used. Primary rat hepatocytes were isolated by collagenase perfusion and cultured as described previously (25). Cell viability in response to chemotherapy was determined by trypan blue exclusion. Rat and human liver mitochondria were isolated as described in Supplementary Methods. Mitochondria from HCC were obtained by rapid centrifugation through Percoll density gradient as described previously (19). Mitoplasts and outer mitochondrial membranes were prepared by the fractionation of rat liver mitochondria with digitonin as described previously (19), monitoring the monoamine oxidase activity for efficiency. In some experiments, the mitochondrial suspension was incubated with 2-(2-methoxyethoxy)ethyl-8-(*cis*-2-*n*-octylcyclopropyl) octane (A_2C, 125 nmol/mg protein) at 37°C for 30 min as described in detail (19).

Human hepatocarcinoma samples. Fresh-frozen samples from tumor lesions were obtained from 6 patients (men, ages 57–73 y) with HC and approved by the ethics committee. The samples were collected from the surgical specimen after resection (n = 2) or from the liver explant at transplantation (n = 4). In four cases, the tumor was multifocal, and in two cases, uninodular. The underlying liver disease was alcoholic cirrhosis in three cases, Hepatitis B virus–induced cirrhosis in two, and Hepatitis C virus–induced cirrhosis in one. In addition, normal liver tissue was obtained from the surgical specimen after partial hepatectomy because of colorectal cancer metastatic to the liver.

Determination of cholesterol and phospholipid levels. The amount of cholesterol in mitochondria was measured by high performance liquid chromatography (HPLC) using a Waters μBondapak C18 10-μm reversed-phase column (30 cm × 4 mm inner diameter; ref. 26). The quantitation of phospholipids is described in detail in the Supplementary Methods.

Immunocytochemistry and laser confocal imaging. Cells were fixed for 10 min with 3.7% paraformaldehyde in 0.1 mol/L phosphate buffer before permeabilization with 0.1% saponin in 0.5% bovine serum albumin (BSA)/PBS buffer for 5 min. Cells were incubated for 1 h with mouse monoclonal antibody anti–cytochrome *c* (1:200; PharMingen), rinsed with PBS, and incubated for 45 min with the secondary antibody. In some cases, filipin (50 μg/mL) was added during the secondary antibody incubation as described before (27). Images were obtained by confocal microscopy as described in Supplementary Methods.

Modulation of cholesterol content and membrane order determination. Cholesterol enrichment was achieved by incubating rat liver mitochondria with a cholesterol-BSA complex at room temperature for 5 min as described (19). Parallel control experiments were performed using only BSA. Cholesterol depletion in mitochondrial membranes from HepG2 or H35 cells was achieved by treatment with Me-β-cyclodextrin (MCD; 40 mmol/L) for 30 min. Mitochondrial membrane order was evaluated by fluorescence anisotropy of the mitochondria-bound dye 1,6-diphenyl-1, 3, 5-hexatriene (DPH) as described previously (17, 19), determining the S_{DPH} from the steady-state fluorescence anisotropy values as described (28).

Silencing of StAR by siRNA. The siRNA-targeting StAR and scrambled siRNA were commercially purchased from Santa Cruz Biotechnology, Inc. Transfection was performed using Lipofectamine2000 (Invitrogen) following the instruction of the manufacturer. Briefly, 5×10^5 HepG2 or H35 cells were incubated with the transfection mixtures containing 100 pmol of the siRNA-targeting StAR or the scrambled control siRNA. Cells were assayed 48 h after transfection for mRNA and protein StAR levels, and for susceptibility to chemotherapy.

HCC xenograft model and treatment. Five- to six-week-old male BALB/c athymic (nu/nu) nude mice were kept under pathogen-free conditions and given free access to standard food and sterilized water. All procedures were performed according to protocols approved by the Institut d'Investigacions Biomèdiques August Pi i Sunyer Ethical Committee. HepG2 cells (2.5×10^6 in 200 μL of PBS) were injected s.c. into the flanks of the mice. Tumors were measured periodically with a vernier caliper, and the volume was calculated as length × width^2 × 0.5, which has been validated previously in comparison with other established methods (29). After 2 to 3 wk, mice were randomly divided into 3 experimental groups: group A, solvent (control); group B, atorvastatin (10 mg/kg); and group C, YM-53601 (15 mg/kg). After 2 wk of daily treatment by p.o. gavage, some animals received an i.p. injection of doxorubicin (10 mg/kg). Differences in tumor volume during the next week were evaluated in each group and expressed as percentage of change in tumor growth with respect to the volume measured before chemotherapy administration.

Terminal deoxynucleotidyl-transferase–mediated dUTP nick-end labeling assay and tumor progression. After sacrifice, tumors were fixed and paraffin sections (5 μm) from each area were stained with terminal deoxynucleotidyl-transferase–mediated dUTP nick-end labeling (TUNEL) reagent using a commercial kit (*In Situ* Cell Death Detection kit; POD from Roche). Immunohistochemical staining of CD34, a specific endothelial cell marker commonly used for microvessel quantification, was performed with rat monoclonal anti-CD34 antibody (Abcam) at a dilution of 1:50 (2 mg/mL). The slices were examined with a Zeiss Axioplan microscope equipped with a Nikon DXM1200F digital camera. Serum α-feto protein levels were measured by the Centro Diagnóstico Médico (Hospital Clinic).

Statistics. Results were expressed as mean ± SD with the number of individual experiments detailed in figure legends. Statistical significance of the mean values was established by the two-tailed distribution Student's t test.

Supplementary methods. This section describes the procedures for Western blot analysis, quantitative real-time PCR, large unilamellar vesicle (LUV) preparation, and fluorimetric assays.

Results

Mitochondrial cholesterol in established HCC. Because previous findings reported enhanced mitochondrial cholesterol content in solid Morris hepatoma tumors with respect to host liver (12–15), we first assessed the mitochondrial cholesterol levels from established HCC. HepG2 and H35 cells were fractionated into mitochondria and analyzed for lipid composition. Electron microscopy and Western blot analysis of PERK, Na^+/K^+ ATPase α1, and Rab5A indicated insignificant contamination with endoplasmic reticulum, plasma membrane, and endosomes, respectively, in the final mitochondrial fraction (Fig. 1*A*). Monitoring Lamp1 levels by Western blot analysis further indicated the lack of lysosomal contamination in the final mitochondrial fraction (Fig. 1*A*). As shown, the total cholesterol levels in mitochondria from H35 and HepG2 cells were 3- to 10-fold higher with respect to rat and human liver mitochondria without changes in total phospholipids content (Fig. 1*B*), confirming previous results in implanted hepatoma tumors *in vivo* (12–15). Interestingly, the levels of mitochondrial cholesterol from primary tumors of patients with HC were higher than the content of mitochondria from nontumor human liver tissue and similar to those found in HepG2 cells (Fig. 1*B*). Moreover, the enhanced levels of free cholesterol of H35 or HepG2 cells examined by confocal microscopy by filipin staining colocalized with mitochondria, and this increase was further verified by HPLC analyses of isolated mitochondria (Fig. 1*C*). Finally, these findings on mitochondrial cholesterol up-regulation correlated with enhanced expression of the transcription factor SREBP-2 and HMG-CoAR in H35 and HepG2 cells with respect to rat and human liver samples (Fig. 1*D*). Together, these findings validate the use of HCC lines to study the role of mitochondrial cholesterol in chemotherapy susceptibility.

HMG-CoAR or squalene synthase inhibition sensitizes HCC to mitochondria-targeted chemotherapy. We next examined the role of mitochondrial cholesterol in the susceptibility of HCC to chemotherapy targeting mitochondria. Arsenic trioxide or lonidamine, a derivative of indazole-3-carboxylic acid, are both antineoplastic drugs that target mitochondria and induce mitochondrial permeability transition (MPT; refs. 30, 31). Thapsigargin-based prodrugs developed for the treatment of prostate cancer (32) are potent inhibitors of endoplasmic reticulum Ca^{2+} ATPases and induce MPT by Ca^{2+} overload, whereas doxorubicin, an anthracycline antibiotic drug, stimulates mitochondrial reactive oxygen species (ROS) generation (33). Both cell lines displayed a reduced susceptibility to increasing doses of thapsigargin, lonidamine, arsenic trioxide, or doxorubicin compared with primary rat hepatocytes (Fig. 2*A*). Various statins including lovastatin or atorvastatin have been shown to be effective in reducing cholesterol levels in HepG2 cells (34). Lovastatin pretreatment sensitized H35 cells to mitochondria-targeting drugs (Fig. 2*B*) with similar results observed with HepG2 cells (Supplementary Fig. S1). Dying cells displayed apoptotic features, such as caspase-3 activation (Supplementary Fig. S2*A*) and chromatin disruption (Supplementary Fig. S2*B*). Moreover, the susceptibility of H35 cells to bafilomycin A, an inhibitor of the vacuolar type H^+-ATPase that impairs lysosomal function and promotes apoptosis independently of MMP (35), was not increased by lovastatin (Supplementary Fig. S1; Fig. 2*B*) and was not accompanied by enhanced cytochrome *c* release (Supplementary Fig. S3), suggesting that the sensitizing effect of lovastatin is specific for mitochondrial-targeting drugs. To further verify the specific role of cholesterol in chemotherapy resistance, we investigated the effect of SS inhibition, which blocks cholesterol biosynthesis without affecting the isoprenoid metabolism (Supplementary Fig. S4). Cell treatment with YM-53601, a specific SS inhibitor (36), at a dose nontoxic to primary rat hepatocytes (Supplementary Fig. S5), potentiated the susceptibility of H35 cells to thapsigargin, lonidamine, and doxorubicin (Fig. 2*C*) to a similar extent as seen by lovastatin treatment. Importantly, both lovastatin and YM-53601 reduced the mitochondrial cholesterol levels in both H35 and HepG2 cells (Fig. 2*D*). Finally, the susceptibility of H35 cells to doxorubicin by lovastatin was prevented by mevalonate, independently of the inhibition of farnesyltransferase, whereas mevalonate failed to restore resistance to doxorubicin after SS inhibition (Supplementary Fig. S6). Moreover, 7-dehydrocholesterol, the immediate precursor of cholesterol synthesis (Supplementary Fig. S4), decreased the susceptibility to doxorubicin by SS inhibition (Supplementary Fig. S6). Collectively, these findings suggest the involvement of mitochondrial cholesterol in the resistance of HCC to drug-induced cell death independently of alterations in isoprenoid metabolism.

siRNA-mediated StAR silencing sensitizes HCC to chemotherapy. To further substantiate that mitochondrial cholesterol enrichment in HCC contributes to mitochondrial-targeting chemotherapy resistance, we investigated the role of silencing StAR. StAR is a cholesterol-transporting polypeptide involved in the intramitochondrial trafficking of cholesterol, which regulates the synthesis of steroids in specialized tissues (11, 16). The levels of StAR were higher in H35 and HepG2 cells compared with rat and human liver samples being more abundant in HepG2 cells than in H35 cells (Fig. 3*A*), which correlated with the mitochondrial cholesterol levels observed in these cell lines (Fig. 1*B*). Transfection with siRNA-targeting StAR resulted in a significant reduction of StAR protein and mRNA expression compared with cells tranfected with scrambled control siRNA (Fig. 3*B*), causing a significant reduction of mitochondrial cholesterol levels (Fig. 3*C*). More importantly, the susceptibility of HepG2 cells to doxorubicin, thapsigargin, or arsenic trioxide was potentiated by transfection with StAR siRNA (Fig. 3*D*), with similar results observed with H35 cells (Fig. 3*D*). Thus, these findings validate the observations with HMG-CoAR and SS inhibition, further supporting a key role for mitochondrial cholesterol in the sensitization of HCC to chemotherapy targeting mitochondria.

Mitochondrial cholesterol modulates membrane order and MPT. Cholesterol, particularly free cholesterol, regulates membrane physical properties (1, 27, 28). Thus, we next determined the membrane order from the steady-state fluorescence anisotropy of DPH-labeled mitochondria. Mitochondria from H35 and HepG2 cells showed higher membrane order (S_{DPH}) compared with mitochondria from rat and human liver (Fig. 4*A*). Phospholipids can also regulate membrane order. However, the content of phosphatidylcholine, the major phospholipid in membranes, remained unchanged in mitochondria from H35 and HepG2 cells with respect to rat or human liver samples, whereas phosphatidylethanolamine levels in mitochondria from HepG2 cells but not H35 cells were slightly lower than those found in human liver mitochondria (Supplementary Fig. S7). Moreover, mitochondria from H35 and HepG2 cells exposed to the cholesterol-binding agent MCD exhibited a significant depletion of cholesterol levels compared with untreated mitochondria, which translated in reduced membrane order (Fig. 4*A*). In contrast, incubation of rat liver mitochondria with a cholesterol-albumin complex (19) resulted in significant cholesterol loading, reaching the levels

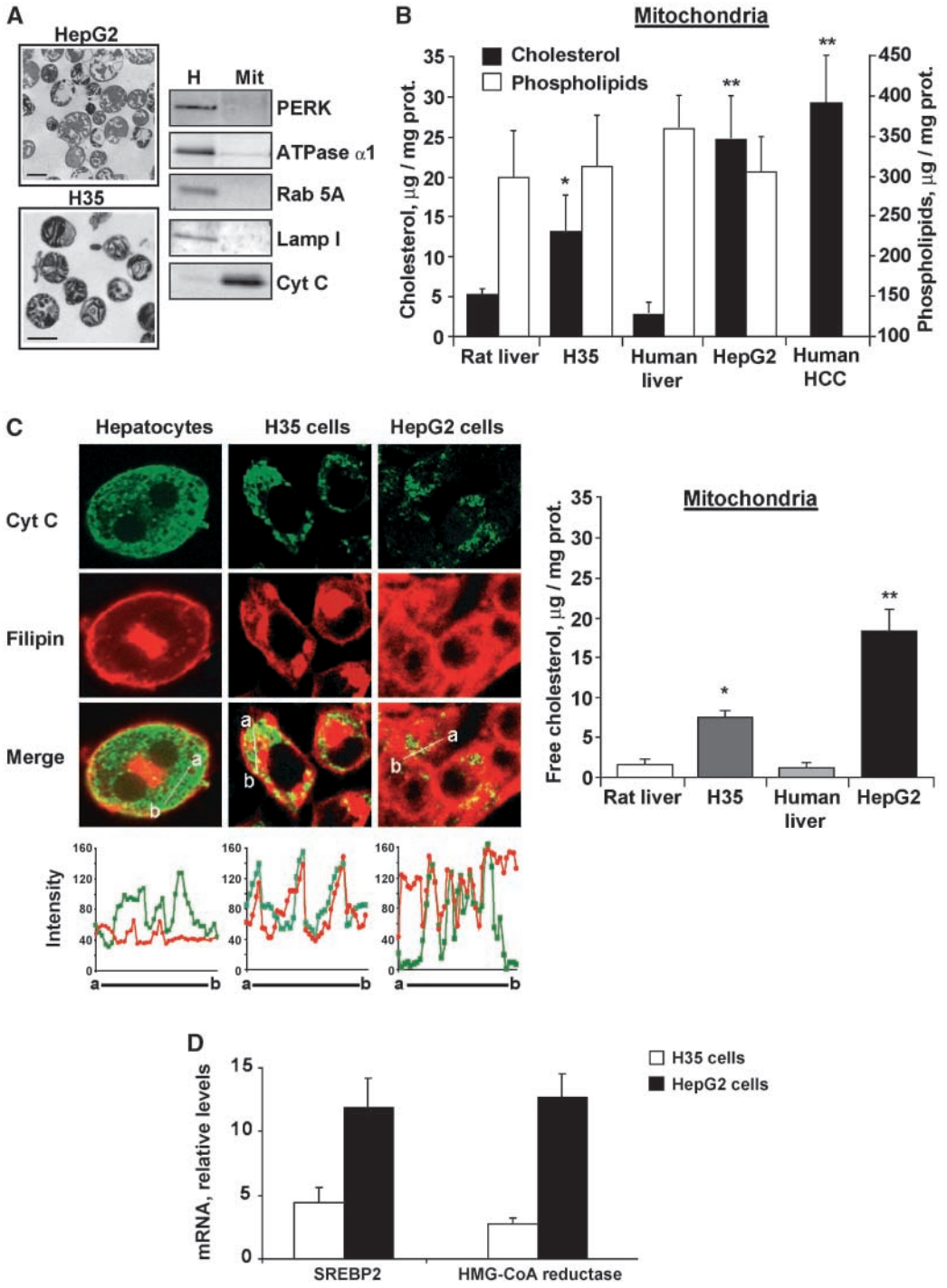

Figure 1. Increased cholesterol content in mitochondria from rat (*H35*), human (*HepG2*) hepatoma cell lines, and human HC samples. *A,* electron microscopy analysis showing purified mitochondria from H35 and HepG2 cells after cellular subfractionation (*scale bars,* 1 μm); and Western blot analysis of PERK, Na^+/K^+ATPase α1, Rab5A, Lamp1, and cytochrome *c* expression in homogenates (*H*) or mitochondrial fraction (*Mit*) from H35 cells. *B,* total cholesterol (*black bars*) and phospholipid levels (*white bars*) performed by HPLC on lipid extracts from the mitochondrial fraction from H35, HepG2 cells, and human HC samples. *C,* colocalization of mitochondria and free cholesterol by confocal microscopy using mouse anti–cytochrome *c* (*cyt C*) and filipin, respectively. The graphs on the bottom represent the fluorescence intensity profiles plotted from a to b direction for the different cell lines. In addition, mitochondrial-free cholesterol content analyzed by HPLC. Results in *B* and *C* are mean ± SD values from at least three independent experiments. * and **, $P < 0.01$ versus rat and human liver mitochondria, respectively. *D,* quantitative real-time reverse transcription-PCR mRNA expression of SREBP-2 and HMG-CoA reductase in H35 and HepG2 cells compared with rat and human liver, respectively. Absolute mRNA values were determined, normalized to hypoxanthine phosphoribosyltransferase and reported as relative levels referred to the expression in nontumor counterpart. *Prot,* protein.

found in mitochondria from H35 cells that increased the membrane order (Fig. 4*A*). Indeed, the mitochondrial membrane order correlated with the cholesterol content (Fig. 4*A*). Cholesterol distribution after cholesterol enrichment by the cholesterol-albumin complex was estimated in mitoplasts. Although the bulk of cholesterol (60–70%) was found in the outer membrane, in agreement with previous findings (19), the levels of cholesterol in mitoplasts from cholesterol-enriched mitochondria were higher (2- to 3-fold) than those found in mitoplasts from control mitochondria (data not shown).

We next analyzed the role of cholesterol in the response of mitochondria to MPT triggers. Isolated mitochondria from H35 cells with or without MCD treatment were incubated with the superoxide anion-generating system, xanthine plus xanthine oxidase (X-XO), shown to induce the release of mitochondrial cytochrome *c* (37). Although rat liver mitochondria released cytochrome *c* in response to X-XO, mitochondria from H35 were resistant to X-XO–induced cytochrome *c* release (Fig. 4*B*); moreover, cholesterol extraction by MCD restored the sensitivity of mitochondria from H35 cells to X-XO–mediated cytochrome *c* release (Fig. 4*B*), with similar findings observed in mitochondria from HepG2 cells (Fig. 4*B*).

Ca^{2+} induces the transition of the MPT pore causing mitochondrial matrix swelling and release of the proapoptotic proteins (38). Rat liver mitochondria enriched in cholesterol by the cholesterol-albumin complex were resistant to swelling (data not shown), and cytochrome *c* and Smac/DIABLO release (Fig. 4*C*) induced by Ca^{2+}. Moreover, mitochondria from H35 cells were insensitive to Ca^{2+}-induced Smac/DIABLO and cytochrome *c* release (Fig. 4*D*), whereas cholesterol depletion by MCD restored the response to Ca^{2+} (Fig. 4*D*). Thus, mitochondrial cholesterol regulates membrane order and the release of apoptotic proteins by MPT triggers.

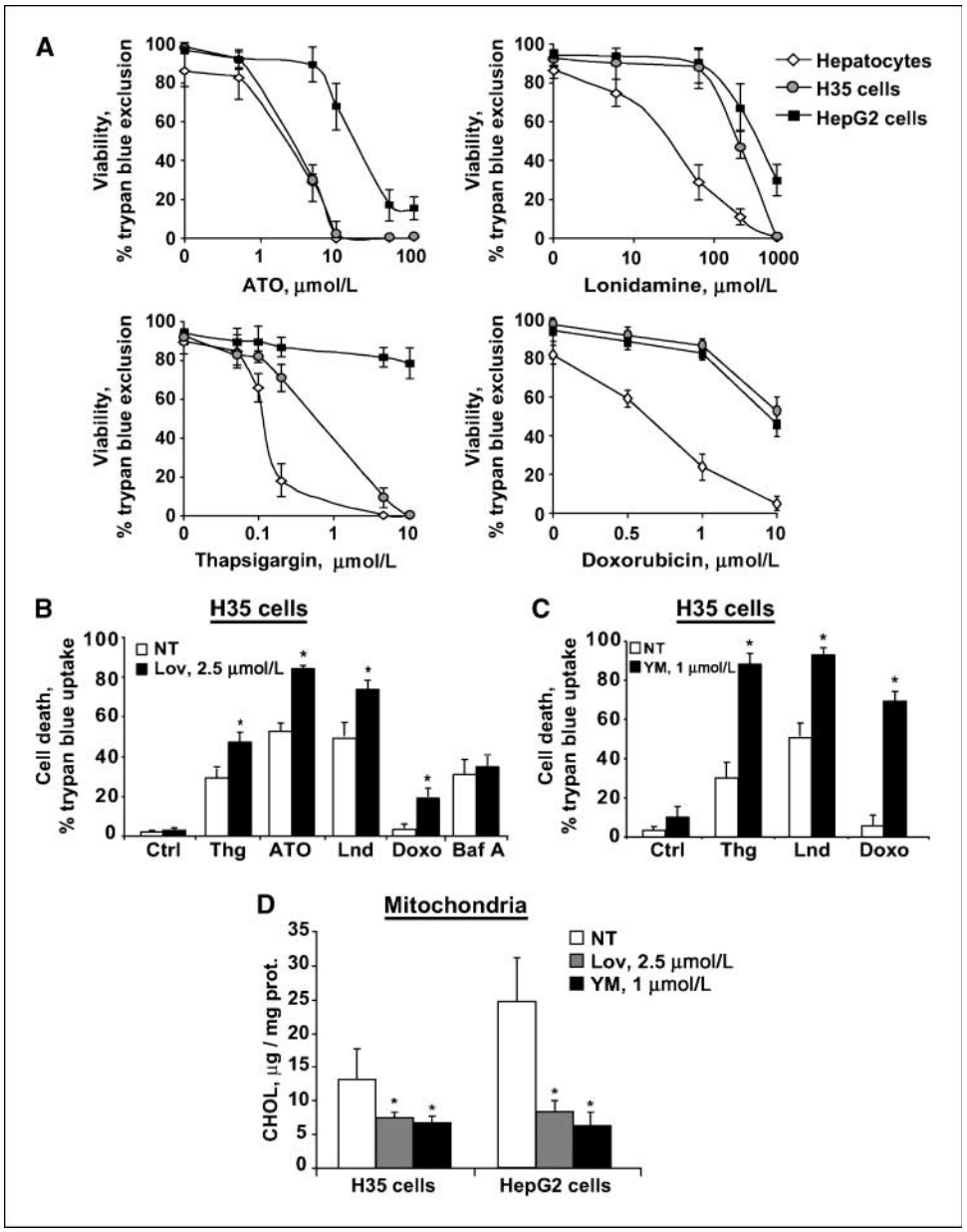

Figure 2. Inhibition of cholesterol synthesis sensitizes cells to different compounds that act on mitochondria. *A,* primary rat hepatocytes, H35, and HepG2 cells were incubated with increasing doses of arsenic trioxide (*ATO*), lonidamine, thapsigargin (*Thg*), or doxorubicin for 24 h. Cell viability was determined by trypan blue exclusion. At least 100 cells in 4 different fields were counted and expressed as a percentage of total cells. *B* and *C,* disruption of cholesterol biosynthesis by lovastain or by the SS inhibitor YM-53601 (*YM*) sensitizes H35 cells to chemotherapeutic agents. H35 hepatoma cells untreated (*NT*) or incubated with lovastatin (*Lov*) or YM-53601 for 24 h were exposed to thapsigargin (0.2 μmol/L), lonidamine (0.2 mmol/L), arsenic trioxide (5 μmol/L), doxorubicin (*Doxo*; 1 μmol/L), bafilomycin A (*Baf A*; 10 μmol/L) for 24 h. Cell death was determined by trypan blue exclusion ($n = 3$). *D,* total cholesterol levels of mitochondria from H35 and HepG2 cells 24 h after treatment with lovastatin (2.5 μmol/L) or YM-53601 (1 μmol/L); $n = 4$; *, $P < 0.05$ versus untreated cells. *Ctrl,* control.

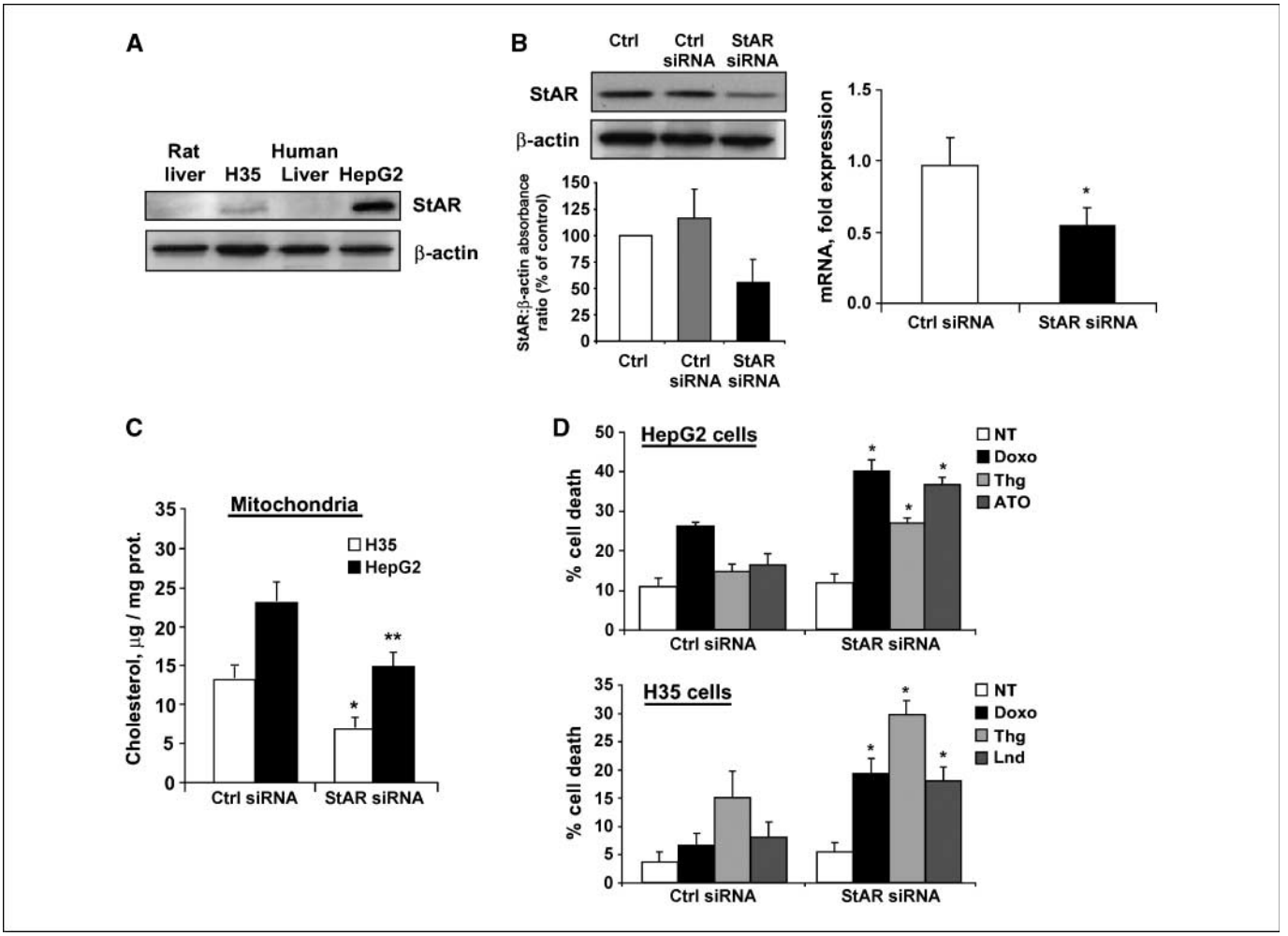

Figure 3. StAR suppression by siRNA increases the cytotoxicity induced by doxorubicin. *A,* representative immunoblot showing StAR protein abundance in H35 and HepG2 cellular extracts and in homogenates from rat and human liver. *B,* StAR mRNA silencing. HepG2 cells were transfected with the StAR siRNA or the control siRNA (*Ctrl siRNA*) as described in Materials and Methods. Cells were allowed to recover in regular culture medium for 48 h, and the levels of StAR protein were quantified by Western blot in cellular extracts (*left*; $n = 3$) and mRNA levels by real-time RT-PCR (*right*; $n = 3$). *C,* mitochondrial cholesterol levels from HepG2 and H35 cells 48 h after StAR mRNA silencing analyzed by HPLC. *D,* 48 h after transfection with StAR or control siRNA, cells were exposed to doxorubicin (1 μmol/L), thapsigargin (0.2 μmol/L), lonidamine (*Lnd*; 0.2 mmol/L), and arsenic trioxide (5 μmol/L), and cell death was analyzed 48 h later by trypan blue exclusion. At least 100 cells in 4 different fields were counted and expressed as a percentage of total cells; $n = 3$; *, $P < 0.05$ versus control siRNA–transfected cells treated with doxorubicin.

Cholesterol impairs Bax-driven mitochondrial release of apoptotic proteins and permeabilization in liposomes. Mitochondrial release of prodeath factors by Bax or Bak can occur by their oligomerization and insertion into the mitochondrial outer membrane independent of MPT (22). Thus, we next examined the effect of cholesterol on Bax-driven mitochondrial permeabilization. Whereas tBid-activated Bax (tBid/Bax) stimulated the release of cytochrome *c* in control mitochondria, cholesterol-enriched mitochondria were resistant to tBid/Bax-mediated cytochrome *c* release (Fig. 5*A*). Similar findings were observed in the release of Smac/Diablo by cholesterol enrichment (data not shown). The incubation of cholesterol-enriched mitochondria with A_2C, a fatty acid derivative that intercalates into the lipid bilayer resulting in its fluidization (19), restored the ability of tBid/Bax to release cytochrome *c* (Fig. 5*A*), establishing a cause-and-effect relationship between mitochondrial membrane order and release of apoptotic proteins by Bax. Moreover, mitochondria from H35 cells were insensitive to tBid/Bax-induced release of cytochrome *c* that was restored by lovastatin treatment (Fig. 5*A*), which caused a significant reduction in the mitochondrial cholesterol levels (Fig. 2*D*).

To further extend these obserations, we next examined the effect of cholesterol on the poration of large unilamellar vesicles (LUVs) by active Bax. LUVs with or without cholesterol were loaded with self-quenching concentrations of FD-70, and the release of LUV-entrapped FD-70 was monitored as an increase in the fluorescence signal due to marker dilution in the external medium (24). As shown, the release of vesicular content by tBid/Bax was impaired in cholesterol-containing LUVs (Fig. 5*B*). In contrast, cholesterol was required for the release of vesicular contents induced by tetanolysin, a cholesterol-dependent pore-forming toxin known to open proteinaceous channels by inserting a transmembrane α-barrel in the bilayer (Fig. 5*B*; ref. 39). Treatment of LUVs with MCD reversed the inhibitory effect of cholesterol upon Bax-driven liposome permeabilization and disrupted the cholesterol-dependent channel-forming function of tetanolysin (Fig. 5*B*). Furthermore, cholesterol inhibited the membrane-permeabilizing activity of tBid/Bax or Bax preoligomerized with octylglucoside (Oligo-Bax)

in a dose-dependent manner (Fig. 5*B*). Similar to the effect found on Bax, and consistent with previous observations, cholesterol also decreased the permeabilizing activity of melittin, a widely studied antimicrobial peptide thought to breach membrane permeability barrier by forming lipid-containing toroidal pores instead of purely proteinaceous channels (40). In contrast, similar to tetanolysin and consistent with previous findings, cholesterol actually increased the release of vesicular contents induced by the channel-forming protein *S. aureaus* α-toxin (Fig. 5*B*; ref. 41). Antiapoptotic proteins such as Bcl-2 antagonize the release of mitochondrial prodeath factors during apoptosis. To address whether cholesterol modulates Bcl-2 activity, LUVs with or without cholesterol were incubated with Bcl-2DC before tBid/Bax treatment. As seen, Bax-driven membrane permeabilization of LUVs was inhibited by Bcl-2DC in a dose-dependent manner, despite the presence of membrane cholesterol (Fig. 5*C*). Consistent with the findings in cholesterol-enriched rat liver mitochondria, the resistance to Bax-induced permeabilization of cholesterol-containing LUVs was reversed by the fluidizing agent A_2C (Fig. 5*D*). Finally, we examined whether cholesterol altered the membrane-inserting capacity of preoligomerized Bax (Oligo-Bax) using lipid monolayers. Addition of oligo-Bax into cholesterol-containing or cholesterol-devoid lipid monolayers at different initial surface pressures allowed us to determine critical surface pressures values (π_0) for oligo-Bax, which is a measure of the membrane penetrability of the protein. As seen, π_0 values for oligo-Bax in cholesterol-containing monolayers were notably lower than in monolayers devoid of cholesterol (Fig. 5*D*). Together, these findings suggest that cholesterol-mediated rigidification of the bilayer directly modulates Bax permeabilizing activity, at least, in part, by reducing the capacity of Bax to insert into the lipid matrix of the membrane.

HMG-CoAR or SS inhibition potentiates chemotherapy in tumor xenografts. We further evaluated whether cholesterol regulates cancer therapy *in vivo* using tumor xenografts. Nude mice were s.c. injected with human hepatoma HepG2 cells, and tumor-bearing animals were then subjected to lipid-lowering treatments.

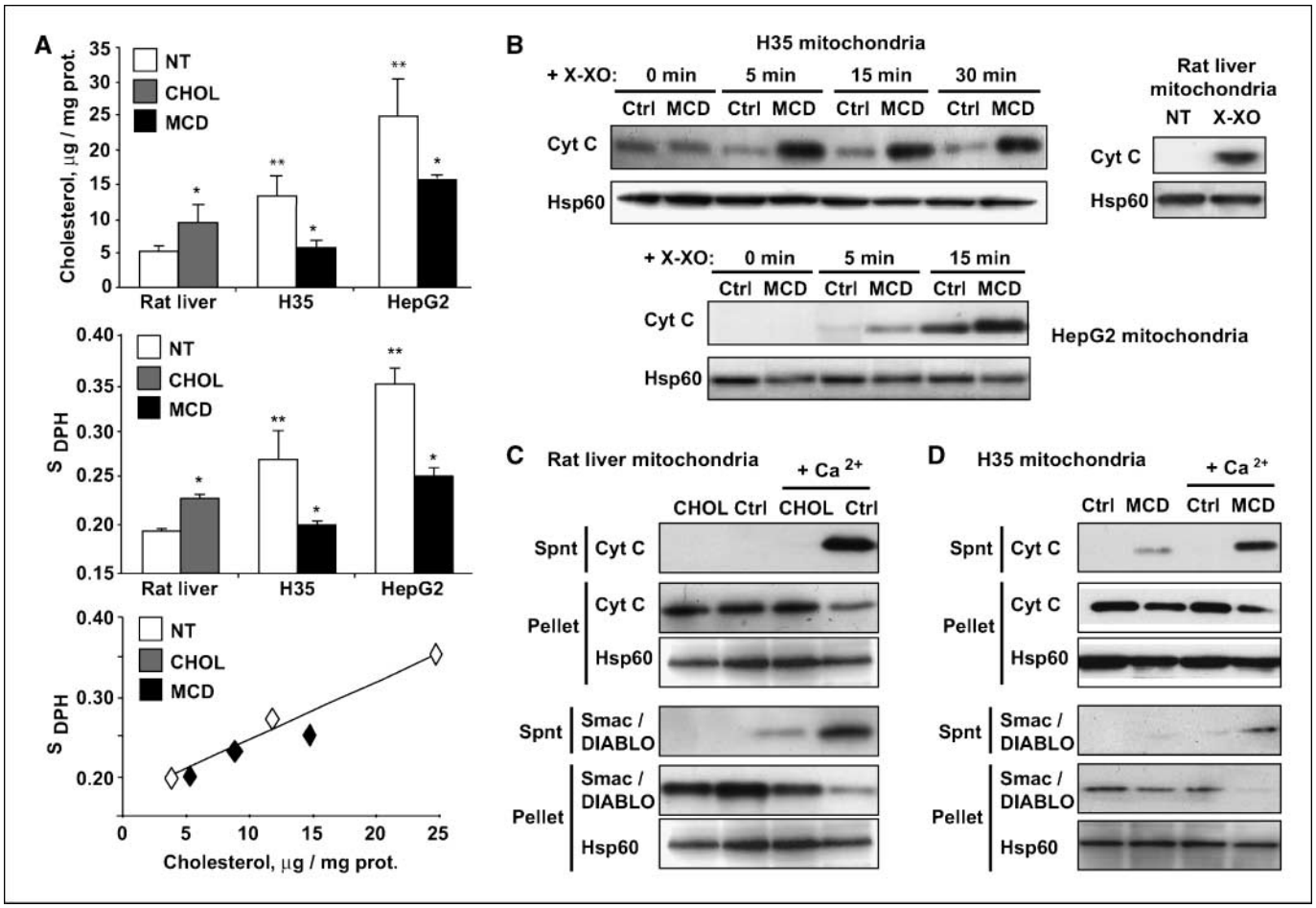

Figure 4. Mitochondrial cholesterol modulation regulates the release of cytochrome *c* and Smac/Diablo by ROS and Ca^{2+}. *A,* total cholesterol levels determined by HPLC of untreated mitochondria or after cholesterol enrichment by a cholesterol-albumin complex (*CHOL*) and Me-β-cyclodextrine treatment (MCD; *top*). *Middle,* membrane order (S_{DPH}) determined from the fluorescence anisotropy monitored at 366 nm (emission, 440 nm) of mitochondria labeled with DPH, using polarizing filters in both excitation and emission planes, and normalized as per milligram of mitochondrial protein.; $n = 3$; *, $P < 0.05$ versus untreated mitochondria; **, $P < 0.05$ versus rat liver mitochondria. *Bottom,* correlation between mitochondrial cholesterol content and membrane order (S_{DPH}). *B,* control and cholesterol-depleted (MCD) mitochondria from H35 and HepG2 cells were incubated with xanthine (0.1 mmol/L) plus xanthine oxidase (40 mU/mL; *X-XO*), and the effect on the release of cytochrome *c* was analyzed by Western blot in the supernatants at the indicated times. Rat liver mitochondria were exposed to X-XO, and the release of cytochrome *c* was analyzed by Western blot in the supernatants. *C,* release of apoptogenic proteins by Ca^{2+} in control and cholesterol-enriched mitochondria from rat liver. Supernatants and pellets from mitochondria with or without $CaCl_2$ (100 μmol/L) treatment for 1 h were used to analyze the levels of cytochrome *c* and Smac/DIABLO. *D,* representative immunoblots of cytochrome *c* and Smac/DIABLO in supernatants and pellets of control and Me-β-cyclodextrin–treated mitochondria from H35 cells, with or without $CaCl_2$ (100 μmol/L) exposure for 30 min. *B* to *D,* the blots shown are representative of 3 to 4 independent experiments showing similar results. The mitochondrial hsp60 protein was visualized as a loading control.

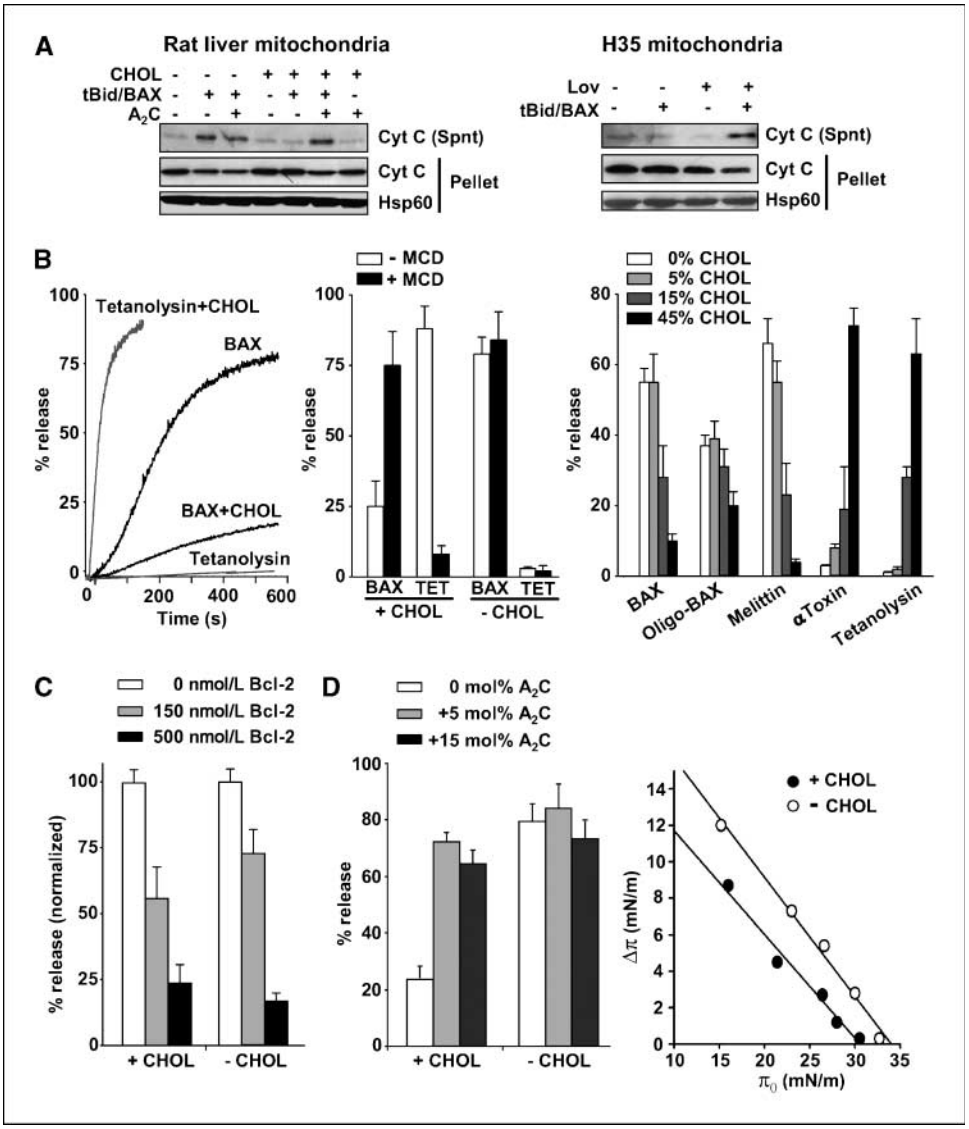

Figure 5. Cholesterol inhibits BAX-driven membrane permeabilization. *A,* representative immunoblots of cytochrome *c* in supernatants and pellets of mitochondria from control and cholesterol-enriched rat liver mitochondria (*CHOL*) with or without A_2C incubation (125 nmol/mg protein) after 45 min of tBid+Bax (20 nmol/L) treatment (*left*). *Right,* representative immunoblots of cytochrome *c* in supernatants and pellets of mitochondria from H35 cells treated or not with lovastatin (2.5 μmol/L) followed by 45 min of tBid+Bax (20 nmol/L) treatment. *B,* representative kinetics of BAX + tBID- (50 nmol/L) and tetanolysin-induced (10 nmol/L) FD70 release from LUV composed of phosphatidylcholine (PC)/cardiolipin (CL) 90/10 (mol/mol; −*CHOL*) or PC/CL/cholesterol 45/10/45 (mol/mol; +*CHOL*; *left*). *Middle,* BAX+tBID- (*BAX*; 50 nmol/L) and tetanolysin-induced (*TET*; 10 nmol/L) FD70 release from LUV, in the presence or absence of 2 mmol/L methyl-β-cyclodextrin MCD ($n = 2$). *Right,* vesicular FD-70 release induced by BAX+tBID (20 nmol/L), BAX oligomerized (*oligo-BAX;* 50 nmol/L), melittin (200 nmol/L), *S. aureaus* α-toxin (α *toxin;* 20 nmol/L), and tetanolysin (5 nmol/L) in LUV composed of PC/CL 90/10 (mol/mol) in which PC was substituted by increasing amounts of cholesterol ($n = 3$–6). *C,* FD-70 release in LUV composed as in *B* and exposed to indicated amounts of Bcl-2 for 5 min before treatment with BAX+tBID (50 nmol/L). The data are normalized as a percentage of the release produced by BAX+tBID in the absence of Bcl-2 ($n = 2$). *D,* dose-dependent effect of A_2C on FD70 release from LUV composed of PC/CL/CHOL 45/10/45 (mol/mol) in which PC was substituted by increasing amounts of A_2C and then exposed to Bax and tBid (50 nmol/L each; *left*). *Columns,* mean two to four independent measurements; *bars,* SD. *Right,* cholesterol reduces the ability of oligomerized Bax by octylglucoside to penetrate into lipid monolayers at different surface pressures. Lipid composition was PC/CL 80/20 (−CHOL) and PC/CL/CHOL 40/20/40 (+CHOL). Critical surface pressures values were 34.6 mN/m (−CHOL) and 30.2 mN/m (+CHOL). Oligomeric Bax concentration was 400 nmol/L.

Atorvastatin was chosen for *in vivo* studies as it has been shown to be more effective than other statins both in humans and experimental animals (42, 43). We observed that both atorvastatin and YM-53601 administration significantly decreased the intratumor cholesterol levels (Fig. 6*A*). No differences in the pattern or in the amount of microvessel formation were observed in any of the experimental groups (Supplementary Fig. S8), suggesting that cholesterol content plays a minor role in tumor vascularization in this xenograft model. However, although atorvastatin notably reduced the size of the tumors or the increase in α-feto protein levels in serum (data not shown) after 2 weeks of administration, such effect was not observed with YM-53601 treatment (Fig. 6*B*), indicating that inhibition of tumor progression by statins may be in part caused by isoprenoids down-regulation, in agreement with previous studies (9, 10). Interestingly, however, mice treated with atorvastatin or the SS inhibitor displayed a greater reduction in tumor growth after doxorubicin administration compared with untreated mice (Fig. 6*C*). Furthermore, a higher number of apoptotic cells assessed by TUNEL staining was observed in tumors from atorvastatin or YM-53601 treated mice after

doxorubicin administration compared with doxorubicin alone (Fig. 6*D*), indicating an increased susceptibility of HCC to the chemotherapeutic agent. Together, these data highlight the potential relevance of the increased mitochondrial cholesterol in modulating the response of HC to chemotherapy *in vivo*.

Discussion

Since its description decades ago in heterotopic Morris hepatoma xenografts in Buffalo rats, the mitochondrial enrichment in cholesterol has been viewed mainly as a key factor underlying, in part, the mitochondrial dysfunction characteristic of cancer cells (7). In this study, however, we investigated the role of cholesterol accumulation in mitochondria from HCC in response to chemotherapy *in vitro* and *in vivo* and the mechanisms involved. First, we confirmed that established human and rat HCC exhibit increased mitochondrial cholesterol levels with respect to nontumor mitochondria of human and rat liver, as reported in solid hepatoma mitochondria compared with host liver (12–15), which paralleled those found in mitochondria from primary tumors of patients with HC. Close to 70% of the cholesterol found in mitochondria from HCC was unsterified, which, in contrast to esterified cholesterol, is known to regulate membrane dynamics and order (1, 2, 19, 27, 28). Moreover, the up-regulation of mitochondrial cholesterol content in HCC correlates with increased expression of SREBP-2 and HMG-CoAR, thus validating the cholesterol deregulation of cancer cells (7–9) and their use to examine the susceptibility to chemotherapy.

Our data uncover the resistance of HCC to chemotherapy-induced cell death that was reversed when cholesterol levels were reduced by inhibition of HMG-CoAR or SS. Although this strategy depletes cholesterol in different types of membranes other than mitochondria such as in specific domains of the plasma membrane, which has been described to modulate cancer therapy by regulating survival pathways such as Akt (5, 6), we provide evidence supporting a specific role for the mitochondrial cholesterol in modulating the susceptibility of HCC to chemotherapy. First, we show that the sensitivity of HepG2 and H35 cells to arsenic trioxide and lonidamine is potentiated by cholesterol depletion by HMG-CoAR or SS inhibition. Arsenic trioxide and lonidamine both induced MPT-mediated apoptosis by targeting the adenine nucleotide translocator (ANT)1 isoform (30, 31). Four ANT isoforms have been described, which are encoded by closely related genes that belong to the mitochondrial carrier family, and ANT is a major component of the MPT that mediate MMP and cell death (44). Mitochondria from murine cells lacking ANT 1 and ANT2 can

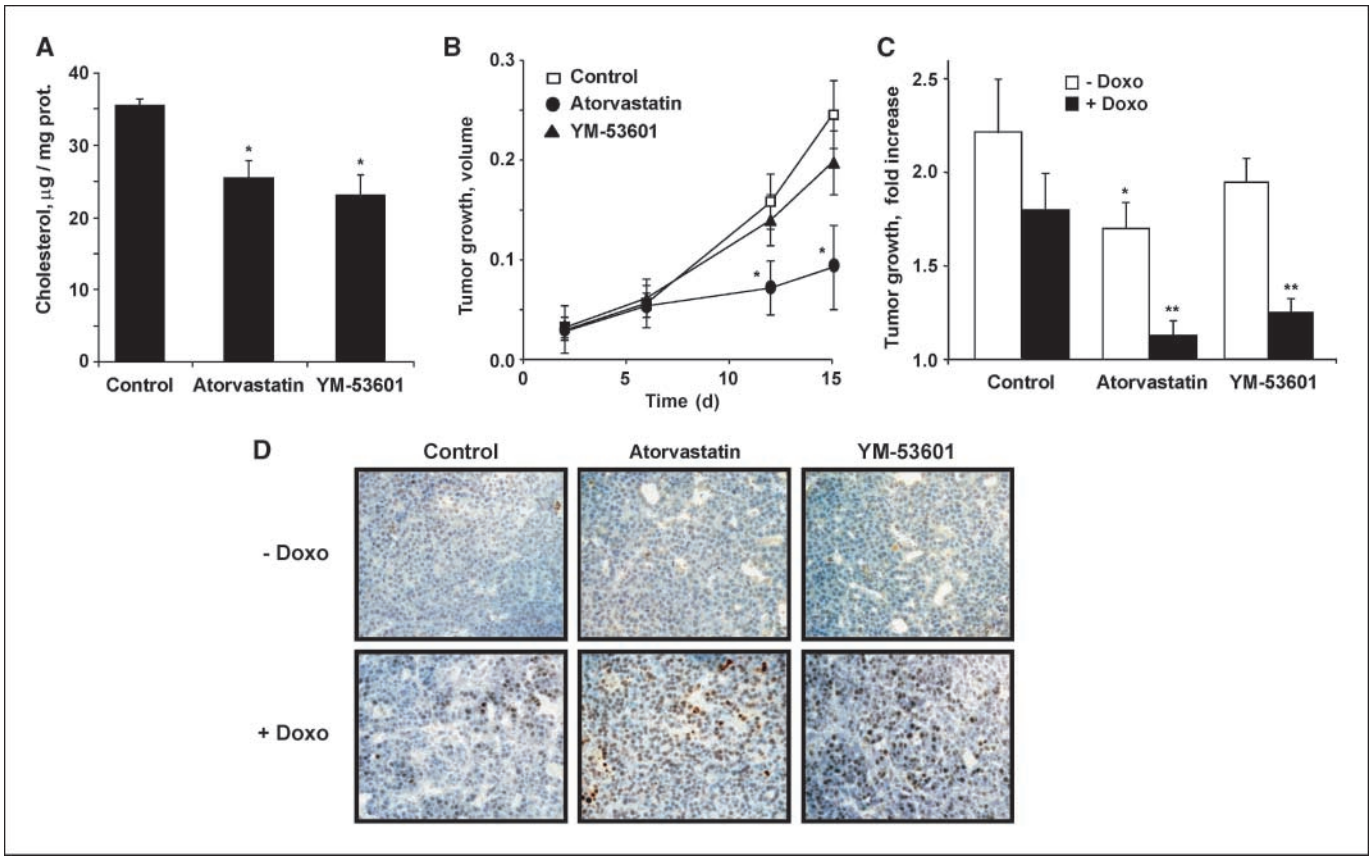

Figure 6. Reduction of cholesterol synthesis potentiates doxorubicin therapy in an *in vivo* murine model. HepG2 cells (2.5×10^6 cells per animal) were implanted s.c. in the flanks of athymic mice as described in Materials and Methods. When tumors averaged 50 mm^3 in size (2–3 wk), mice were randomly divided into the experimental groups and treated by a daily p.o. gavage with atorvastatin (10 mg/kg body weight) or YM-53601 (15 mg/kg body weight) for 2 wk. *A,* cholesterol levels from control (vehicle treated), atorvastatin, and YM-53601–treated tumors ($n = 5$). *, $P < 0.05$ versus control. *B,* tumor growth measured periodically at the indicated days over the treatment. The volume was calculated as length $\times$ width$^2 \times 0.5$. The experiment was performed twice with similar results. *, $P < 0.05$ versus vehicle-treated tumor. *C,* after 2 wk of treatment, some animals received an i.p. injection of doxorubicin (10 mg/kg). Fold increase of tumor growth was evaluated in each experimental group ($n = 5$) by calculating the changes in tumor size observed after administration of the chemotherapy agent. The experiment was performed twice with similar results. *, $P < 0.05$ versus doxorubicin-treated control mice. *D,* apoptosis induced by the chemotherapy agent in tumors from animals treated either with statins or SS inhibitor was analyzed by TUNEL-positive staining areas. Representative images of three samples per group performed showing similar results.

still undergo Ca^{2+}-induced swelling and MPT, although at a higher threshold (45), which have been viewed as evidence against a role for ANT in MPT and hence in MMP. However, the ability of ANT1/ANT2-deficient cells to undergo MMP might be due to the functional compensation by a novel ANT isoform identified recently (46) or by other mitochondrial carriers able to form pores in the inner membrane, such as the ornithine/citrulline transporters or the phosphate carrier (47).

Furthermore, additional evidence for a role of mitochondrial cholesterol in chemotherapy susceptibility derives from the outcome observed by StAR silencing. StAR is a polypeptide responsible for the intramitochondrial transport of cholesterol (11, 16) and both HepG2 and H35 cells overexpress StAR levels. StAR silencing by siRNA sensitizes these cell lines to chemotherapy-induced cell death. Consistent with its role in the mitochondrial trafficking of cholesterol, the sensitization to chemotherapy by StAR down-regulation could reflect impaired cholesterol transport from the outer to the inner mitochondrial membranes. However, our data indicate that StAR depletion by siRNA resulted in the net decrease of mitochondrial cholesterol levels, implying lower delivery of cholesterol to mitochondria from extramitochondrial sources by other proteins including (StAR)-related lipid transfer (StART) family members. Although the molecular mechanisms of StAR are poorly understood, recent findings have shown that StAR interacts with specific outer mitochondrial membrane proteins such as VDAC1 and the phosphate carrier protein (48). Whether StAR works in concert with other StART members via interaction with specific proteins of the outer mitochondrial membrane to deliver cholesterol to mitochondria remains to be investigated. Thus, collectively, these data strongly suggest that the enrichment of mitochondria in cholesterol plays a role in the resistance of chemotherapy acting via mitochondria.

To explore the mechanism of the mitochondrial cholesterol–mediated resistance to chemotherapy, we focused on the membrane properties of isolated mitochondria from HCC. We observed that mitochondria from HepG2 and H35 cells exhibit higher order which is reversed by cholesterol extraction with MCD or fluidization by A_2C, translating in increased MMP and release of cytochrome *c* and Smac/Diablo in response to Ca^{2+}, superoxide anion, and active Bax. An important piece of evidence supporting the specificity of cholesterol in the regulation of MMP is the fact that the *in vitro* enrichment of rat liver mitochondria in cholesterol to about the same levels seen in H35 cells reproduces the resistance to MMP and release of intermembrane apoptotic proteins induced by active Bax. Consistent with these observations, cholesterol-containing LUVs are also resistant to the poration induced by Bax, and cholesterol dose-dependently inhibited the vesicular release induced by melittin, which has been proposed to permeabilize membranes by forming toroidal lipidic pores (40). Because positive monolayer curvature stress contributes to MMP by Bax (24), it is conceivable that cholesterol may stabilize mitochondrial membranes against Bax permeabilizing action through induction of negative curvature, consistent with the accumulation of cholesterol in high-curvature regions of membranes (49). Remarkably, cholesterol decreased the capacity of Bax to penetrate into the membrane, which is considered to be a critical step in Bax activation. Thus, through modulation of membrane order and curvature stress, cholesterol may regulate Bax activity and the formation of lipidic pores in mitochondrial membranes and, hence, cell death susceptibility.

We also observed that tumor growth and chemotherapy susceptibility in heterotopic murine tumor xenografts were modulated by HMG-CoAR or SS inhibition, with both strategies decreasing tumor mitochondrial cholesterol levels. The generation of farnesyl diphosphate from mevalonate branches into isoprenoids and squalene, which is then committed for cholesterol synthesis (Supplementary Fig. S4). Isoprenoids are known to modify the function of proteins through posttranslational modifications such as the Rho family of small GTPases that coordinates many aspects of cell motility through the reorganization of actin cytoskeleton and changes in gene transcription (9, 10). The isoprenylation is essential for Rho-mediated invasion of various tumors, including melanoma, pancreatic, and breast cancer cells (50). In the *in vivo* xenograft model, we observed that HMG-CoAR but not SS reduced tumor growth, suggesting that inhibition of tumor progression by statins may be in part caused by isoprenoids down-regulation. However, the susceptibility of HC xenografts to chemotherapy are observed upon statins or SS inhibition, supporting the relevance of cholesterol rather than isoprenoids generation in the resistance of HCC to chemotherapy. Thus, our findings regarding the role of SS inhibition on chemotherapy along with recent reports in different types of cancer cells such as human prostate carcinoma cell lines (51) highlight the relevance of cholesterol modulation in cancer therapy.

Interestingly in line with our data, recent findings in liposomes confirmed that mitochondrial Bax activation is inhibited by cholesterol (52). Moreover, mitochondria from HeLa cells treated with U18666A, which caused mitochondrial cholesterol up-regulation, showed a delay in the release of Smac/Diablo and cytochrome *c*, as well as in Bax oligomerization and partial protection against stress-induced apoptosis (52).

In summary, although enhanced cholesterol levels in cell membranes including mitochondria from cancer cells have been long known, we show here for the first time the relevance of the cholesterol-mediated regulation of mitochondrial membrane dynamics in the response of HCC to mitochondrial-targeting chemotherapy *in vitro* and *in vivo*. Moreover, the potentiation of HC chemotherapy by SS inhibition, which reduces cholesterol levels including in mitochondria, without perturbing isoprenoid metabolism, validates the specificity of cholesterol in chemotherapy resistance, and revitalizes the potential benefit of cholesterol down-regulation in cancer therapy.

Disclosure of Potential Conflicts of Interest

No potential conflicts of interest were disclosed.

Acknowledgments

Received 11/8/2007; revised 3/14/2008; accepted 4/16/2008.

Grant support: Research Center for Liver and Pancreatic Diseases Grant P50 AA 11999 funded by the US National Institute on Alcohol Abuse and Alcoholism; Plan Nacional de I+D Grants SAF2005-03923, SAF2005-03943, SAF2006-06780, BFU2005-06095, and FIS06/0395; the Centro de Investigacion Biomedica en Red de Enfermedades Hepaticas y Digestivas supported by the Instituto de Salud Carlos III; the Ramon y Cajal Research Program (Ministry of Education and Science; A. Colell and A. Morales); and a predoctoral fellowship from the Basque Government (O. Terrones).

The costs of publication of this article were defrayed in part by the payment of page charges. This article must therefore be hereby marked *advertisement* in accordance with 18 U.S.C. Section 1734 solely to indicate this fact.

We thank Susana Nuñez for the technical assistance and Dr. Bataller for the donation of human liver samples; Virginia Villar from Clinic and Center for Applied Medical Research, Pamplona, for her assistance in providing human HC samples; and the Servicio Cientifico-Técnico of IDIBAPS for electron microscopy, confocal imaging, and flow cytometry analysis.

References

1. Maxfield FR, Tabas I. Role of cholesterol and lipid organization in disease. Nature 2005;438:612–21.
2. Gimpl G, Burger K, Fahrenholz F. Cholesterol as modulator of receptor function. Biochemistry 1997;36: 10959–74.
3. Simons K, Ehehalt R. Cholesterol, lipid rafts, and disease. J Clin Invest 2002;110:597–603.
4. Horton JD, Goldstein JL, Brown MS. SREBPs: activators of the complete program of cholesterol and fatty acid synthesis in the liver. J Clin Invest 2002;109: 1125–31.
5. Zhuang L, Kim J, Adam RM, Solomon KR, Freeman MR. Cholesterol targeting alters lipid raft composition and cell survival in prostate cancer cells and xenografts. J Clin Invest 2005;115:958–68.
6. Li YC, Park MJ, Ye S-K, Kim C-W, KimY-N. Elevated levels of cholesterol-rich lipid rafts in cancer cells are correlated with apoptosis sensitivity induced by cholesterol-depleting agents. Am J Pathol 2006;168:1107–18.
7. Siperstein MD. Cholesterol, cholesterogenesis and cancer. Adv Exp Med Biol 1995;369:155–66.
8. Duncan RE, El-Sohemy A, Archer MC. Mevalonate promotes the growth of tumors derived from human cancer cells *in vivo* and stimulates proliferation *in vitro* with enhanced cyclin-dependent kinase-2 activity. J Biol Chem 2004;279:33079–84.
9. Demierre MF, Higgins PDR, Gruber SB, Hawk E, Lippman SM. Statins and cancer prevention. Nat Rev Cancer 2005;5:930–42.
10. Liao JK, Laufs U. Pleiotropic effects of statins. Annu Rev Pharmacol Toxicol 2004;45:89–118.
11. Soccio RE, Breslow JL. Intracellular cholesterol transport. Arterioscler Thromb Vasc Biol 2004;24:1150–60.
12. Feo F, Canuto RA, Bertone G, Garcea R, Pani P. Cholesterol and phospholipid composition of mitochondria and microsomes isolated from morris hepatoma 5123 and rat liver. FEBS Lett 1973;33:229–32.
13. Crain RC, Clark RW, Harvey BE. Role of lipid transfer proteins in athe abnormal lipid content of Morris hepatoma mitochondria and microsomes. Cancer Res 1983;43:3197–202.
14. Campbell AM, Capuano A, Chan SHP. A cholesterol-binding and transporting protein from rat liver mitochondria. Biochim Biophys Acta 2002;1567:123–32.
15. Feo F, Canuto RA, Garcea R, Gabriel L. Effect of cholesterol content on some physical and functional properties of mitochondria isolated from adult rat liver, fetal liver, cholesterol-enriched liver and hepatomas AH-130, 3924A and 5123. Biochim Biophys Acta 1975; 413:116–34.
16. Hall EA, Ren S, Hylemon PB, et al. Detection of the steroidogenic acute regulatory protein, StAR, in human liver cells. Biochim Biophys Acta 2005;1733:111–19.
17. Colell A, García-Ruiz C, Morales A, et al. Transport of reduced glutathione in hepatic mitochondria and mitoplasts from ethanol-treated rats: effect of membrane physical properties and S-adenosyl- L-methionine. Hepatology 1997;26:699–708.
18. Coll O, Colell A, Garcia-Ruiz C, Kaplowitz N, Fernandez-Checa JC. Sensitivity of the 2-oxoglutarate carrier to alcohol intake contributes to mitochondrial glutathione depletion. Hepatology 2003;38:692–702.
19. Colell A, García-Ruiz C, Lluis JM, Coll O, Marí M, Fernández-Checa, JC. Cholesterol impairs the adenine nucleotide translocator-mediated mitochondrial permeability transition through altered membrane fluidity. J Biol Chem 2003;278:33928–35.
20. Baggetto LG, Clottes E, Vial C. Low mitochondrial proton leak due to high membrane cholesterol content and cytosolic creatine kinase as two features of the deviant bioenergetics of Ehrlich and AS30-D tumor cells. Cancer Res 1992;52:4935–41.
21. Galluzzi L, Larochette N, Kroemer G. Mitochondria as therapeutic targets for cancer chemotherapy. Oncogene 2006;5:4812–30.
22. Green DR. At the gates of death. Cancer Cell 2006;9: 328–30.
23. Motola-Kuba D, Zamora-Valdes D, Uribe M, Mendez-Sanchez M. Hepatocellular carcinoma. An overview. Ann Hepatol 2006;5:16–4.
24. Terrones O, Antonsson B, Yamaguchi H, et al. Lipidic pore formation by the concertad action of proapoptotic Bax and tBid. J Biol Chem 2004;279:30081–91.
25. Mari M, Colell A, Morales A. Acidic sphingomyelinase downregulates the liver-specific methionine adenosyltransferase 1A, contributing to tumor necrosis factor-induced lethal hepatitis. J Clin Invest 2004;113:895–904.
26. Duncan IW, Culbreth PH, Burtis CA. Determination of free, total, and esterified cholesterol by high-performance liquid chromatography. J Chromatogr 1979;162:281–92.
27. Mari M, Caballero F, Colell A, et al. Mitochondrial free loading sensitizes to TNF and Fas mediated steatohepatitis. Cell Metab 2006;4:185–98.
28. Van Blitterswijk WJ, van Hoeven RP, van der Meer B.W. Lipid structural order parameters (reciprocal of fluidity) in biomembranes derived from steady-state fluorescence polarization measurements. Biochim Biophys Acta 1981;644:323–32.
29. Hudd C, Euhus DM, LaRegina MC, Herbold DR, Palmer DC, Johnson FE. Effect of cholescytokinin on human cholangiocarcinoma xenografted into nude mice. Cancer Res 1985;45:1372–6.
30. LeBras M, Borgne-Sanchez A, Touat Z, et al. Chemosensitization by knockdown of adenine nucleotide translocase-2. Cancer Res 2006;66:9143–52.
31. Don AS, Kisker O, Dilda P, et al. A peptide trivalent arsenical inhibits tumor angiogenesis by perturbing mitochondrial function in angiogenic endothelial cells. Cancer Cell 2003;3:497–509.
32. Denmeade SR, Isaacs JT. The SERCA pump as a therapeutic target: making a "smart bomb" for prostate cancer. Cancer Biol Ther 2005;4:14–22.
33. Kumar D, Kirshenbaum L, Li T, Danelisen I, Signal P. Apoptosis in isolated adult cardiomyocytes exposed to adriamycin. Ann N Y Acad Sci 1999;874:156–68.
34. Scharnagal H, Schinker R, Gierens H, Nauck M, Wieland H, März W. Effect of atorvastatin, simvastatin and lovastatin on the metabolism of cholesterol and triacylglycerides in HepG2 cells. Biochem Pharmacol 2001;62:1545–55.
35. Hishita T, Tada-Oikawa S, Tohyama K, et al. Caspase-3 activation by lysosomal enzymes in cytochrome c-independent apoptosis in myelodysplastic syndrome-derived cell line P39. Cancer Res 2001;61:2878–84.
36. Ugawa T, Kakuta H, Moritani H, et al. YM-53601, a novel squalene synthase inhibitor, reduces plasma cholesterol and triglyceride levels in several animal species. Br J Pharmacol 2000;131:63–70.
37. Madesh M, Hajnoczky G. VDAC-dependent permeabilization of the outer mitochondrial membrane by superoxide induces rapid and massive cytochrome c release. J Cell Biol 2001;155:1003–15.
38. Ichas F, Mazat JP. From calcium signaling to cell death: two conformations for the mitochondrial permeability transition pore. Switching from low- to high-conductance state. Biochim Biophys Acta 1998; 1366:33–50.
39. Rottem S, Cole RM, Habid WH, Barile MF, Hardegree MC. Structural characteristics of tetanolysin and its binding to lipid vesicles. J Bacteriol 1982;152:888–92.
40. Allende D, Simon SA, Mcintosh TJ. Melittin-induced bilayer leakage depends on lipid material properties: evidence for toroidal pores. Biophys J 2005;88:1828–37.
41. Forti S, Menestrina G. Staphylococcal α-toxin increases the permeability of lipid vesicles by cholesterol- and pH-dependent assembly of oligomeric channels. Eur J Biochem 1989;181:767–73.
42. Jones P, Kafonek S, Laurora I, Huninghake D. Comparative dose efficacy study of atorvastatin versus simvastatin, pravastatin, lovastatin and fluvastatin in patients with hypercholesterolemia (the CURVES study). Am J Cardiol 1998;81:582–87.
43. Auerback BJ, Krause BR, Bisgaier CL, Newton RS. Comparative effects of HMG-CoA reductase inhibitors on apo B production in the casein-fed rabbit: atovastatin versus lovastatin. Atherosclerosis 1995;115:173–80.
44. Halestrap AP, Brenner C. The adenine nucleotide translocator: a central component of the mitochondrial permeability transition pore and key player in cell death. Curr Med Chem 2003;10:1507–25.
45. Kokoszka R, Waymire KG, Levy SE, et al. The ADP/ATP translocator is not essential for the mitochondrial permeability transition pore. Nature 2004;427:461–5.
46. Dolce V, Scarcia P, Iacopetta D, Palmieri F. A fourth ADP/ATP carrier isoform in man: identification, bacterial expression, functional characterization and tissue distribution. FEBS Lett 2005;579:633–7.
47. Palmieri F. The mitochondrial transporter family (SLC25): physiological and pathological implications. Pfluggers Arch 2004;447:689–709.
48. Bose M, Whittal RM, Miller L, Bose HS. Steroidogenic activity of StAR requires contact with mitochondrial VDAC1 and PCP. J Biol Chem 2008;14:8837–45.
49. Wang W, Yang L, Huang HW. Evidence of cholesterol accumulated in high curvature regions: implication to the curvature elastic energy for lipid mixtures. Biophys J 2007;92:2819–30.
50. Collisson EA, Kleer C, Wu M, et al. Atorvastatin prevents RhoC isoprenylation, invasion, and metastasis in human melanoma cells. Mol Cancer Ther 2003;2: 941–48.
51. Brusselmans K, Timmermans L, Van de Sande T, et al. Squalene synthase: A determinant of raft-associated cholesterol and modulator of cancer cell proliferation. J Biol Chem 2007;282:18777–85.
52. Lucken-Ardjomande S, Montessuit S, Martinou JC. Bax activation and stress-induced apoptosis delayed by the accumulation of cholesterol in mitochondrial membranes. Cell Death Differ 2008;15:484–93.

Mitochondrial Cholesterol Contributes to Chemotherapy Resistance in Hepatocellular Carcinoma

Joan Montero, Albert Morales, Laura Llacuna, et al.

Cancer Res 2008;68:5246-5256.